Dynamic magnetic behavior of $BaCoO_3$ quasi-one-dimensional perovskite

P. M. Botta,[1,*] V. Pardo,[1,2] D. Baldomir,[1,2] C. de la Calle,[3]
J. A. Alonso,[3] and J. Rivas[1]
[1]*Departamento de Física Aplicada, Facultad de Física, Universidad de Santiago de Compostela, E-15782 Campus Sur s/n, Santiago de Compostela, Spain*
[2]*Instituto de Investigaciones Tecnológicas, Universidad de Santiago de Compostela, E-15782, Santiago de Compostela, Spain*
[3]*Instituto de Ciencia de Materiales de Madrid, CSIC, Campus de Cantoblanco, 28049-Madrid, Spain*
(Received 24 February 2006; revised manuscript received 31 May 2006; published 15 December 2006)

Polycrystalline $BaCoO_3$ was synthesized by a citrate technique using thermal treatments at high oxygen pressure. Magnetic susceptibility measurements were carried out at very low ac and dc fields on the compound. The magnetic properties of the material between 14 and 30 K were identified with the appearance of nanoscale ferromagnetic regions. The observed magnetic irreversibilities can be understood in the framework of a superparamagnetic model. The real and imaginary parts of the complex susceptibility are consistent with an Arrhenius-like thermal relaxation law with an energy barrier of about 0.05 eV. Through this model, the mean size of the ferromagnetic clusters could be determined; it is about 1 nm in diameter, if spherical geometry is assumed for them.

DOI: 10.1103/PhysRevB.74.214415 PACS number(s): 75.20.−g, 73.22.−f, 75.50.Tt

I. INTRODUCTION

Co oxides have drawn considerable attention in the last few years due to their interesting electronic structure and magnetic properties, such as colossal magnetoresistance,[1] phase separation,[2] aging[3] and memory[4] effects, glassy behavior,[5] superconductivity,[6] spin state,[7] and metal-insulator transitions.[8] In particular, the properties of $BaCoO_3$ have been thoroughly studied recently. The first studies on the material concluded that its ground state was a long-range antiferromagnet.[9–11] However, more recent works showed that its magnetic properties were more complicated and a competition between antiferromagnetic (AF) and ferromagnetic (FM) interactions was observed.[12] On the other hand, electronic structure calculations[13] yielded the ground state of the compound as a long-range ferromagnet with alternating orbital order along the CoO_6 chains (the material has a quasi-one-dimensional structure).

The study of phase-separated transition metal oxides has drawn enormous attention in the last few years. This phenomenon is believed to be at the heart of the understanding of colossal magnetoresistance and it has been found in a wide variety of oxides. Phase separation in the series $Sr_xBa_{1-x}CoO_3$ was predicted theoretically in recent works.[14,15] Analysis of the susceptibility measurements performed by Yamaura *et al.*,[12] combined with *ab initio* electronic structure calculations, have explained the magnetic properties of $BaCoO_3$ by assuming the material is formed by FM regions of a nanometric size embedded in a non-FM matrix. FM droplets have also been recently found in other cobalt oxides,[16] and similar phase separation on a nanometric scale has been thoroughly studied for the case of manganites.[17,18] However, it is still under debate whether such phase separation occurs in $BaCoO_3$. Recent studies[19,20] conclude that, at temperatures lower than 14 K, the material and other related compounds exhibit a two-dimensional AF long-range ordering as evidenced by muon spectroscopy and at T between 14 and 50 K, a one-dimensional FM ordering is deduced from their magnetic susceptibility and specific heat data.

In the present paper we have performed measurements under dc and ac magnetic fields with the aim of bringing more experimental evidence about the occurrence of magnetic phase separation in this system. The obtained experimental results will allow us to characterize the FM clusters, determining their size, relaxation times, and energy barrier. The paper will be organized as follows. In Sec. II, the experimental techniques and the characterization of the sample will be given, in Sec. III the magnetic susceptibility under ac and dc low applied fields will be presented and discussed, and finally, in Sec. IV, the conclusions of our work will be detailed.

II. EXPERIMENTAL TECHNIQUES

$BaCoO_3$ material was obtained in powder form by a citrate technique. Stoichiometric amounts of analytical grade $Ba(NO_3)_2$ and $Co(NO_3)_2 \cdot 6H_2O$ were dissolved in citric acid. The solution was slowly evaporated, leading to an organic resin that was dried at 120 °C and slowly decomposed at temperatures up to 600 °C for 12 h. The black precursor powders, very reactive, after an intermediate treatment at 900 °C in air were heated at 900 °C under 200 bar oxygen pressure for 10 h. Then, the sample was cooled at 300 °C h^{-1} down to room temperature in order to favor the oxygenation of the products. The reaction product was characterized by x-ray diffraction (XRD) for phase identification and to assess phase purity. X-ray analysis was performed using a Bruker-axs D8 diffractometer (40 kV, 30 mA), controlled by DIFFRACT^{plus} software, in Bragg-Brentano reflection geometry with Cu $K\alpha$ radiation ($\lambda = 1.5418$ Å). A secondary graphite monochromator allowed the complete removal of Cu $K\beta$ radiation. The data were obtained between 10° and 100° 2θ in steps of 0.05°. The slit system was selected to ensure that the x-ray beam was completely within the sample at all angles of 2θ.

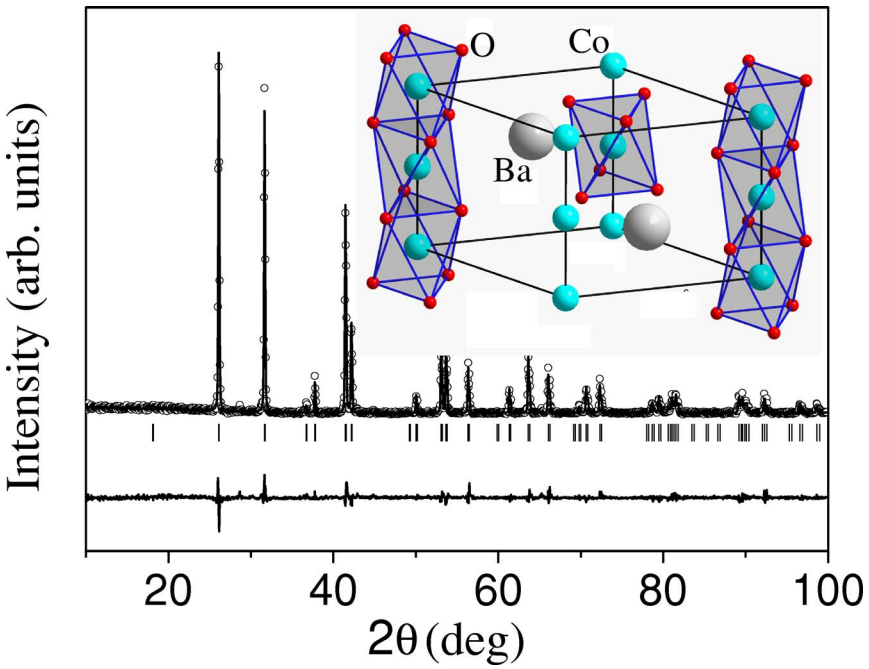

FIG. 1. (Color online) XRD pattern for the synthesized $BaCoO_3$ powder. The good fit between the experimental (circles) and calculated (solid line) profiles confirms the high quality of the sample. The inset shows a sketch of the structure taken from Ref. 13. Observe the quasi-one-dimensional structure formed by CoO_6 chains.

XRD patterns were analyzed by the Rietveld method,[21] using the FULLPROF refinement program.[22] No regions were excluded in the refinement. A pseudo-Voigt function was chosen to generate the line shape of the diffraction peaks. The following parameters were refined in the final run: scale factor, background coefficients, zero-point error, pseudo-Voigt function corrected for asymmetry parameters, positional coordinates, and isotropic thermal factors.

The magnetization (M) between 5 and 320 K was measured in a superconducting quantum interference device magnetometer (Quantum Design) under dc and ac applied fields. For dc experiments, magnetic fields (H) between 25 and 1000 Oe were applied. The magnetization data were taken upon heating in both zero-field-cooling (ZFC) and field-cooling (FC) regimes. ac measurements under ZFC conditions were carried out with an applied field amplitude of 8 Oe at frequencies between 1 and 10 kHz. Also, curves of magnetization as a function of the applied field at constant temperature were recorded.

III. RESULTS AND DISCUSSION

The XRD pattern of $BaCoO_3$ compound is characteristic of a perovskite, showing well-defined reflections corresponding to a hexagonal structure, as is displayed in Fig. 1. No impurity phases were detected. The crystal structure refinement was performed from XRD data collected at room temperature (RT). The structure was defined in the hexagonal space group $P6_3/mmc$ (No. 194). The lattice parameters are $a=5.6525(2)$ Å and $c=4.7629(3)$ Å, and the unit-cell volume is $V=131.79(1)$ Å^3. Ba, Co, and O atoms were located at the $2d$, $2a$, and $6h$ positions, respectively. A good fit between the observed and the calculated profiles was obtained, as is shown in Fig. 1. Table I lists the refined structural and thermal parameters, together with unit-cell parameters refined from XRD data at RT. Table II includes the mean interatomic distances and some selected bond angles. As shown in Table II, Ba–O distances—in the BaO_{12} polyhedron—display an average ⟨Ba–O⟩ value of 2.91 Å that compares well with the expected value from ionic radii (i.r.) sums[23] of 3.01 Å for $^{XII}Ba^{2+}$ (i.r.: 1.61 Å) and $^{VI}O^{2-}$ (i.r.: 1.40 Å). For the cobalt-to-oxygen bonds, the average distance of 1.90 Å is in good agreement with that expected, 1.93 Å, for $^{VI}Co^{4+}$ ions (i.r.: 0.53 Å

$BaCoO_3$ presents a 2H-type perovskite structure, consisting of infinite chains of CoO_6 face-sharing octahedra, running along the c direction. The sharing of faces is associated

TABLE I. Structural parameters for $BaCoO_3$ refined in the hexagonal $P6_3/mmc$ space group from XRD data at RT. Lattice parameters are $a=5.6525$ Å, $c=4.7629$ Å, and the unit-cell volume is $V=131.79$ Å^3. Reliability factors are $\chi^2=1.70$ and $R_{Bragg}\%=6.24$.

Atom	Site	x	y	z	f_{occ}	B (Å)^2
Ba	$2d$	1/3	2/3	3/4	1.0	0.39(9)
Co	$2a$	0	0	0	1.0	0.23(7)
O	$6h$	0.1505(4)	−0.1505(4)	1/4	1.0	0.11(5)

TABLE II. Main bond distances and selected angles for hexagonal $BaCoO_3$ determined from XRD data at RT.

BaO_{12}	Distance (Å)
Ba—O (×6)	2.979(5)
Ba—O (×6)	2.831(8)
CoO_6 octahedra	
Co—O (×6)	1.895(7)
	Angle (deg)
Co—O—Co	77.9 (3)

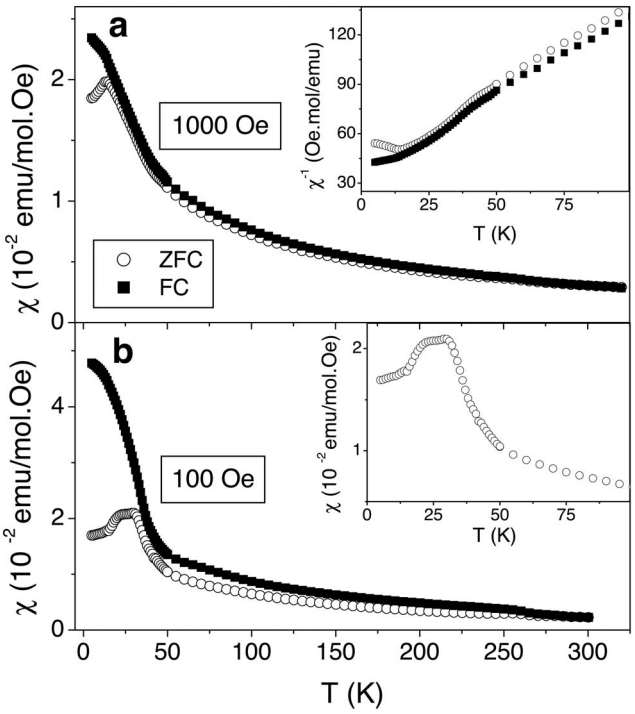

FIG. 2. dc magnetic susceptibility vs temperature at $H=1000$ and 100 Oe. The inset in the upper panel shows the variation of inverse susceptibility at low temperatures. In the bottom panel an enlargement of the ZFC curve around T_B is displayed.

with short metal-metal separations (in this case, Co–Co, 2.381(4) Å) accounting for abnormal magnetic or electrical properties. In a purely ionic crystal, we should expect strong repulsion between Co^{4+} ions at this short distance. However, the O–O distance in shared faces is only 2.543(2) Å; suggesting that the Co^{4+} ions are shielded one from another along the c direction.

Figure 2 shows the magnetic susceptibility as a function of temperature at 1000 and 100 Oe [Figs. 2(a) and 2(b) respectively]. At low temperatures, a peak can be noticed in the ZFC curves of both figures. This cusp is clearly displaced to lower temperatures for higher applied fields, indicating that it is not due to a true magnetic phase transition. Also, in FC curves, a significant increase of χ below this temperature can be noticed. The presence of a peak in χ at lower temperatures for higher magnetic fields resembles the typical response of a system composed of superparamagnetic particles.[24] At a low enough temperature (the so-called blocking temperature, T_B) these particles undergo a blocking indicated by a peak in the ZFC curves and a splitting of the ZFC and FC curves below T_B. In our case, the observed magnetic behavior is due to magnetic or electronic inhomogeneities and not to a real dispersion of small particles. The sudden rise of χ exhibited by the FC curve below T_B suggests that the FM clusters are weakly interacting, in contrast to the typical behavior shown by a spin-glass system. The coexistence of two electronic phases in related systems has been proposed earlier to explain the magnetic response of similar compounds, such as $La_{1-x}Sr_xCoO_3$ and $Ba_5Co_5O_{14}$.[16,25,26]

The inset of Fig. 2(a) shows the inverse susceptibility at $H=1000$ Oe. Besides a change in the sign of the slope at 14 K (corresponding to the blocking of the superparamagnetic clusters), a decrease of the positive slope can be noticed at about 45 K for both ZFC and FC curves. Sugiyama *et al.*[19] have reported the same behavior at similar temperatures ($T=53$ K); they attributed it to a one-dimensional (1D) FM order. According to our physical description,[14] this could indicate an incipient coupling of the magnetic moments of the superparamagnetic clusters, that is blocked at lower temperatures. Considering the structural anisotropy of $BaCoO_3$, it seems reasonable to suppose that the FM 1D ordering experimentally found[19] has to do with the clusters being highly nonspherical. The inset of Fig. 2(b) clearly shows a change in the slope of the ZFC curve at $T \simeq 14$ K. Recently, experiments performed by muon spin rotation and relaxation (μ^+SR) proved that at 14 K a 2D AF transition takes place,[19] suggesting that the anomaly detected at 14 K in the ZFC curve [Fig. 2(b)] could be attributed to this magnetic transition. A careful analysis of this curve reveals that the peak corresponding to the blocking centered at 26.5 K is indeed an overlapping of peaks, suggesting the presence of clusters with different sizes. The overall width of this peak can be estimated as 6 K, leading to a size distribution as narrow as 0.5 nm, assuming spherical geometry for the clusters [see below, Eq. (2)].

Measurements carried out at 25 and 50 Oe do not reveal further increase in T_B and, hence, they are not displayed here. According to Néel's model of superparamagnetism,[27] there exists a maximum blocking temperature, that is reached when the applied field is much lower than the so-called anisotropy field. On the other hand, there is a competition between the disordered regime and the Zeeman energy and, in fact, strong enough magnetic fields can destroy entirely the spin-disordered state. In this way, we can assume that the T_B obtained at 100 Oe is the highest T_B for this system. All our results will be given for these low applied fields and the corresponding T_B.

The measurements carried out at low magnetic fields allow us to observe an interesting feature in the magnetic behavior of $BaCoO_3$. For $H \leqslant 100$ Oe, a large irreversibility between ZFC and FC below 260 K is found. At applied magnetic fields higher than 100 Oe, this feature disappears, showing an almost complete overlapping of both curves. This response has already been reported for this compound, where a paramagnetic state was only found from 260 K on.[12,14] The marked splitting of the ZFC and FC curves suggests that upon cooling the disordered magnetic moments of the Co ions will begin to order in superparamagnetic structures, which are blocked below 30 K. In this way, the following magnetic regimes can be distinguished: for $T<14$ K a 2D AF ordering; for $14\ \text{K}<T<T_B$ a blocked state of the weakly interacting clusters; for $T_B<T<260$ K a fully reversible regime of a superparamagnetic behavior of these nanostructures; and for $T>260$ K paramagnetism of Co^{4+} ions.

Effective magnetic moments (μ_{eff}) were estimated from inverse susceptibility measured at 100 Oe under a ZFC regime assuming a Curie-Weiss behavior. At temperatures between 50 and 200 K, i.e., in the superparamagnetic state, this

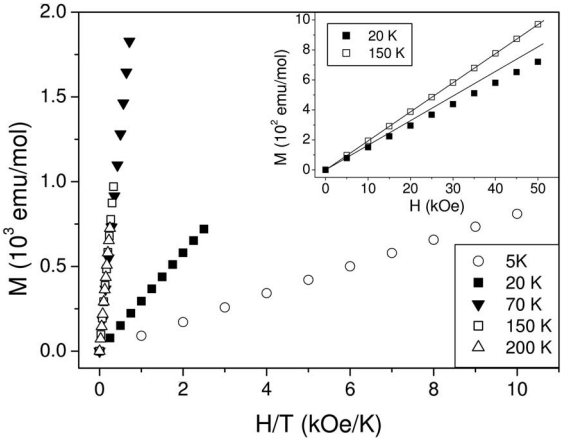

FIG. 3. M vs H/T curves measured at temperatures between 5 and 200 K. The inset shows a deviation from linearity below T_B.

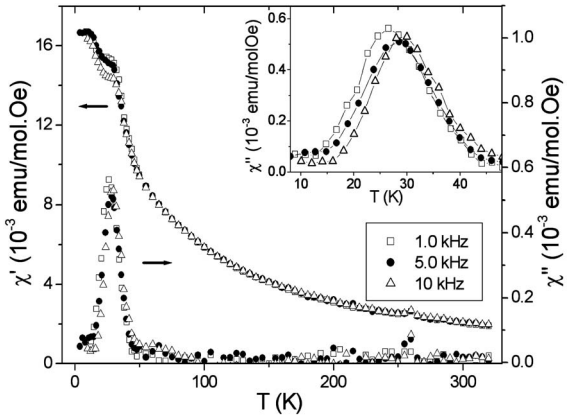

FIG. 4. ac magnetic susceptibility vs temperature at various frequencies. The inset clearly shows that the χ'' peak is shifted to higher temperatures for higher frequencies.

gives $\mu_{eff}=2.5\mu_B$, in good agreement with previously reported values.[19] However, when the temperature is higher than 260 K the effective magnetic moment drops to values very close to that corresponding to single Co^{4+} ions in low-spin state ($\mu_{eff}=1.73\mu_B$) supporting our assertion that a paramagnetic state occurs above this temperature.

Figure 3 shows M vs H/T curves measured at temperatures lower and higher than T_B. Straight lines corresponding to the Langevin expression (superparamagnetism) at relatively low temperatures and moderate magnetic fields can be observed. However, the marked difference in the slope of the curves measured at temperatures lower and higher than T_B is noticeable. The line becomes steeper as temperature increases, reaching a maximum slope at T_B. At higher temperatures all the lines show identical slope, which is consistent with the superparamagnetic state existing in this thermal range. M vs H curves at 20 and 150 K are presented in the inset of Fig. 3. At 150 K, a linear dependence can be observed, wich is expected for a superparamagnetic behavior. In contrast, at 20 K (below the blocking temperature), the curve tends to saturate at the highest applied fields (above some 3×10^4 Oe), evidencing the FM nature of the blocked clusters.

In order to deepen in the physical characteristics of the FM inhomogeneities present in the solid, ac magnetic susceptibility was measured as a function of temperature (Fig. 4). A cusp at a temperature close to 30 K is observed in both real and imaginary parts of the magnetic susceptibility (χ' and χ''). For increasing frequencies, this peak appears at higher temperatures, as shown in the inset of Fig. 4 (for the sake of clarity, only curves at 1, 5, and 10 kHz are displayed). Also, all the curves corresponding to χ' collapse only above 30 K, showing a clear splitting around T_B. These observations support the idea of freezing processes associated with small-size clusters of ferromagnetically ordered regions with temperature. At temperatures close to 260 K, a very small peak in χ' and χ'' can be detected. At this temperature, the splitting of ZFC and FC curves starts, as registered by dc measurements (see Fig. 2). Contrarily to the cusp observed at low temperatures, the position of the peak is insensitive to frequency variations. This suggests a clear change in the magnetic behavior, not related to any relaxation phenomenon, consistent with being the onset of a true magnetic phase transition.

Thermal relaxation of the FM clusters is consistent with an Arrhenius-like law

$$\tau = \tau_0 \exp(Q/kT) \tag{1}$$

where τ is the relaxation time at temperature T, τ_0 is the relaxation time at infinite temperature, Q is the energy barrier, and k is the Boltzmann constant. This energy barrier for the thermal relaxation of the clusters can be estimated to be due to the anisotropy energy associated with each cluster, KV, where K is the magnetic anisotropy constant and V is the mean volume of the cluster. Considering the highly anisotropic structure of $BaCoO_3$, the constant K can be considered to be due mainly to the magnetocrystalline anisotropy energy.[14]

From the experimental data measured in ac experiments, it is possible to obtain the relaxation time (through the employed frequency ν, which is $\nu=1/2\pi\tau$) for each T_B. This is plotted in Fig. 5 with a fit to Eq. (1). A very good linear fit is obtained for the measured data, corroborating the validity of

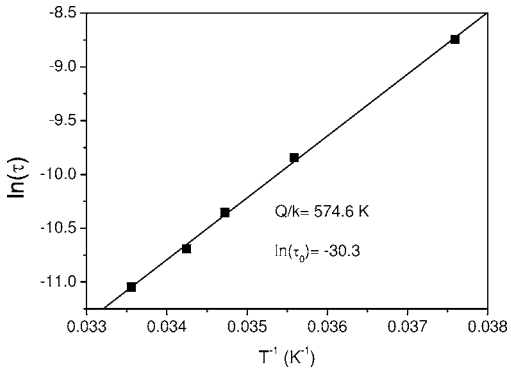

FIG. 5. Linear fit of experimental data obtained for the thermal relaxation of the ferromagnetic clusters, according to Eq. (1). The values calculated for the slope (Q/k) and intercept ($\ln\tau_0$) are displayed.

our hypotheses. The energy barrier can be calculated from the slope of the line, giving $Q=7.9\times10^{-14}$ erg ($\simeq$0.05 eV), which is a reasonable value if we consider those reported for magnetic nanoparticles.[28]

In order to estimate the mean volume of the clusters we will use the value of the anisotropy constant that comes out of the magnetocrystalline anisotropy energy calculated *ab initio* in Ref. 14: $K=2\times10^8$ erg/cm^3. This gives a mean volume of the clusters of about 4×10^{-22} cm^3, i.e., a typical diameter of each cluster of approximately 1 nm, assuming spherical geometry for them. This value is in very good agreement with the results obtained recently by some of us (1.2 nm),[14] where the experimental dc data from Yamaura *et al.*[12] were analyzed. In that case, no measurement of the relaxation times was available and the size was calculated through the following equation, which is valid for superparamagnetic particles:

$$KV = 25kT_B \tag{2}$$

where the factor 25 is associated with the measuring time,[29] assumed with a time constant of 100 s for both ZFC and FC experiments. Also, in Ref. 14, T_B is estimated as the temperature where the ZFC and FC curves separate from each other at 1000 Oe showing the blocking effects. However, if the measurements are carried out at lower fields, it can be observed that such a separation occurs at much higher temperatures, where no blocking effect occurs. We observe that the application of Eq. (2) to our current experimental data with $T_B\simeq30$ K gives a cluster diameter of 1 nm, in excellent agreement with the values of the relaxation times obtained from ac measurements, showing the validity of such a simple expression for our superparamagnetic clusters.

The intercept of the straight line obtained in Fig. 5 provides us with an estimation of τ_0, being about 10^{-13} s. This value is very small compared to those reported by Dormann *et al.*,[24] which are on the order of 10^{-11} s. However, these higher values are obtained for noninteracting nanoparticles of a much bigger size than our clusters, which contain only a few Co ions, and, hence, shorter relaxation times are expected in our case.

IV. CONCLUSIONS

In this paper we present consistent experimental evidence that supports the hypothesis of a phase separation in $BaCoO_3$. Such phase separation is characterized by the appearance of single-domain FM clusters of a nanometric size developing in a non-FM matrix. ac magnetic measurements confirm that for $14<T<30$ K the magnetic properties of the material are governed by relaxation phenomena and not by a true magnetic phase transition. Also, we were able to estimate the size of these regions, which is about 1 nm in diameter. The thermal relaxation of the system could be fitted by an Arrhenius-like equation, with an energy barrier of 0.05 eV. In order to corroborate this magnetic behavior for $BaCoO_3$, small-angle neutron scattering measurements should be performed on this compound. This technique could allow the measurement of the correlation length of these magnetic clusters.

ACKNOWLEDGMENTS

This work was partially funded by the Spanish Ministry of Science and Education of Spain (MEC) under Project Nos. MAT2004-05130-C02-01 and MAT2004-0479. P.M.B. thanks the MEC for financial support under the program J. de la Cierva. V.P. wishes to thank the Xunta de Galicia for financial support.

*Electronic address: pbotta@usc.es

[1] C. Martin, A. Maignan, D. Pelloquin, N. Nguyen, and B. Raveau, Appl. Phys. Lett. **71**, 1421 (1997).
[2] M. J. R. Hoch, P. L. Kuhns, W. G. Moulton, A. P. Reyes, J. Wu, and C. Leighton, Phys. Rev. B **69**, 014425 (2004).
[3] V. G. Prokhorov, Y. P. Lee, K. W. Kim, V. M. Ishchuk, and I. N. Chukanova, Appl. Phys. Lett. **80**, 2353 (2002).
[4] A. Pautrat, H. W. Eng, and W. Prellier, Phys. Rev. B **72**, 233405 (2005).
[5] J. Mira, J. Rivas, K. Jonason, P. Nordblad, M. P. Breijo, and M. A. Señarís-Rodríguez, J. Magn. Magn. Mater. **196-197**, 487 (1999).
[6] K. Takada, H. Sakurai, E. Takayama-Muromachi, F. Izumi, R. A. Dilanian, and T. Sasaki, Nature (London) **422**, 53 (2003).
[7] M. A. Korotin, S. Yu. Ezhov, I. V. Solovyev, V. I. Anisimov, D. I. Khomskii, and G. A. Sawatzky, Phys. Rev. B **54**, 5309 (1996).
[8] C. Frontera, J. L. García-Muñoz, A. Llobet, and M. A. G. Aranda, Phys. Rev. B **65**, 180405(R) (2002).
[9] Y. Takeda, J. Solid State Chem. **15**, 40 (1975).
[10] G. A. Candela, A. H. Kahn, and T. Negas, J. Solid State Chem. **7**, 360 (1973).
[11] M. Shimada, Y. Takeda, H. Taguchi, F. Kanamaru, and M. Koizumi, J. Cryst. Growth **29**, 75 (1975).
[12] K. Yamaura, H. Zandbergen, K. Abe, and R. Cava, J. Solid State Chem. **146**, 96 (1999).
[13] V. Pardo, P. Blaha, M. Iglesias, K. Schwarz, D. Baldomir, and J. E. Arias, Phys. Rev. B **70**, 144422 (2004).
[14] V. Pardo, J. Rivas, D. Baldomir, M. Iglesias, P. Blaha, K. Schwarz, and J. E. Arias, Phys. Rev. B **70**, 212404 (2004).
[15] V. Pardo, J. Rivas, and D. Baldomir, Appl. Phys. Lett. **86**, 202507 (2005).
[16] D. Phelan, D. Louca, S. Rosenkranz, S. H. Lee, Y. Qiu, P. J. Chupas, R. Osborn, H. Zheng, J. F. Mitchell, J. R. D. Copley, J. L. Sarrao, and Y. Moritomo, Phys. Rev. Lett. **96**, 027201 (2006).
[17] E. L. Nagaev, *Colossal Magnetoresistance and Phase Separation in Magnetic Semiconductors* (Imperial College Press, London, 2002).
[18] E. Dagotto, *Nanoscale Phase Separation and Colossal Magnetoresistance* (Springer, Berlin, 2003).

[19] J. Sugiyama, H. Nozaki, J. H. Brewer, E. J. Ansaldo, T. Takami, H. Ikuta, and U. Mizutani, Phys. Rev. B **72**, 064418 (2005).
[20] J. Sugiyama, H. Nozaki, Y. Ikedo, K. Mukai, D. Andreica, A. Amato, J. H. Brewer, E. J. Ansaldo, G. D. Morris, T. Takami, and H. Ikuta, Phys. Rev. Lett. **96**, 197206 (2006).
[21] H. M. Rietveld, J. Appl. Crystallogr. **2**, 65 (1969).
[22] J. Rodríguez-Carvajal, Physica B **192**, 55 (1993).
[23] R. D. Shannon, Acta Crystallogr., Sect. A: Cryst. Phys., Diffr., Theor. Gen. Crystallogr. **32**, 751 (1976).
[24] J. L. Dormann, D. Fiorani, and E. Tronc, Adv. Chem. Phys. **98**, 283 (1997).
[25] M. A. Señarís Rodríguez, and J. B. Goodenough, J. Solid State Chem. **118**, 323 (1995).
[26] K. Boulahya, M. Parras, J. M. González-Calbet, U. Amador, J. L. Martínez, V. Tissen, and M. T. Fernández-Díaz, Phys. Rev. B **71**, 144402 (2005).
[27] L. Néel, Ann. Geophys. (C.N.R.S.) **5**, 99 (1949).
[28] J. L. Dormann, F. D'Orazio, F. Lucari, E. Tronc, P. Prené, J. P. Jolivet, D. Fiorani, R. Cherkaoui, and M. Noguès, Phys. Rev. B **53**, 14291 (1996).
[29] A. H. Morrish, *The Physical Principles of Magnetism* (IEEE Press, New York, 2001).